HHS Public Access

Author manuscript

Sci Immunol. Author manuscript; available in PMC 2022 February 13.

Published in final edited form as:

Sci Immunol. 2021 August 13; 6(62): . doi:10.1126/sciimmunol.abi5586.

Clonally expanded, GPR15-expressing pathogenic effector T_H2 cells are associated with eosinophilic esophagitis

Duncan M. Morgan[1,2], **Bert Ruiter**[3,4], **Neal P. Smith**[3], **Ang A. Tu**[1,5,6], **Brinda Monian**[1,2], **Brandon E. Stone**[3], **Navneet Virk-Hundal**[7], **Qian Yuan**[7], **Wayne G. Shreffler**[3,4,7], **J. Christopher Love**[1,2,8,9]

[1]Koch Institute for Integrative Cancer Research, MIT, Cambridge, MA, USA

[2]Department of Chemical Engineering, MIT, Cambridge, MA, USA

[3]Center for Immunology & Inflammatory Diseases, Massachusetts General Hospital, Boston, MA, USA

[4]Harvard Medical School, Boston, MA, USA

[5]Department of Biological Engineering, MIT, Cambridge, MA, USA

[6]Immunitas Therapeutics Inc. Cambridge, MA, USA

[7]Food Allergy Center, Massachusetts General Hospital, Boston, MA, USA

[8]Broad Institute of MIT and Harvard, Cambridge, MA, USA

[9]Ragon Institute of MGH, MIT, and Harvard, Cambridge, MA, USA

Abstract

Eosinophilic esophagitis (EoE) is an allergic disorder characterized by the recruitment of eosinophils to the esophagus, resulting in chronic inflammation. We sought to understand the cellular populations present in tissue biopsies of patients with EoE and to determine how these populations are altered between active disease and remission. To this end, we analyzed cells obtained from esophageal biopsies, duodenal biopsies, and peripheral blood of EoE patients in active disease or remission with single-cell RNA and TCR sequencing. Pathogenic effector T_H2 (peT_H2) cells present in the esophageal biopsies of patients with active disease expressed distinct gene signatures associated with the synthesis of eicosanoids. The esophageal tissue-resident peT_H2 population also exhibited clonal expansion, suggesting antigen-specific activation. Peripheral CRTH2+CD161- and CRTH2+CD161+ memory CD4+ T cells were enriched for either a conventional T_H2 phenotype or a peT_H2 phenotype, respectively. These cells also exhibited

Author contributions: W.G.S., J.C.L., D.M.M., and B.R. conceptualized the study. Q.Y. and N.V. performed clinical work. D.M.M, B.R., N.P.S, and B.E.S. conducted experiments. D.M.M., A.A.T., and B.M. performed bioinformatic analyses. D.M.M., B.R., W.G.S., and J.C.L. wrote and edited the manuscript.

Competing interests: W.G.S., J.C.L., D.M.M., and B.R. are inventors on a pending patent application at Massachusetts General Hospital that covers the results presented in this manuscript. W.G.S. serves on the S.A.B of Aimmune Therapeutics, Allergy Therapeutics, FARE and is a consultant for ALK, Merck, Nestle, Novartis, Regeneron, and Sanofi. J.C.L. is an advisor and co-founder of Honeycomb Biotechnologies. J.C.L.'s interests are reviewed and managed under MIT's policies for potential conflicts of interests.

Data and materials availability: Whole transcriptome and TCR sequencing data from esophageal biopsies, duodenal biopsies, and peripheral blood is available on GEO, accession number GSE175930. Source data files for figures and analysis is available at github.com/duncanmorgan/EoE_SciImmunol or Zenodo (10.5281/zenodo.5047633).

substantial clonal expansion and convergence of TCR sequences, suggesting that peripheral peT$_H$2 cells are expanded in response to a defined set of antigens. The esophagus-homing receptor *GPR15* was upregulated by peripheral peT$_H$2 clonotypes that were also detected in the esophagus. Lastly, GPR15+ peT$_H$2 cells were enriched among milk-reactive CD4+ T cells in patients with milk-triggered disease, suggesting that these cells are an expanded, food antigen-specific population with enhanced esophagus homing potential.

One Sentence Summary

T$_H$2 cells in eosinophilic esophagitis exhibit clonotypic features of an antigen-specific response and enhanced esophagus-homing ability.

Introduction

Eosinophilic esophagitis (EoE) is an allergic disease characterized by chronic esophageal inflammation with prominent recruitment of eosinophils, resulting in difficulty swallowing, food impaction, and esophageal dysfunction (1, 2). Clinically, EoE often manifests as an antigen-specific disease, in which exposure to specific food-derived allergens triggers esophageal inflammation (3), but evidence for an antigen-specific adaptive immune response in EoE is lacking. Inflammation in EoE involves T helper (T$_H$) 2 cells that produce the cytokines IL-5, which promotes eosinophil recruitment and activation, and IL-13, which exacerbates epithelial barrier dysfunction (4–6). Much of the available transcriptional and genetic data, however, appear to place dysregulation of an epithelial unit at the center of disease pathogenesis (6–8). In addition, while patients with EoE exhibit increased numbers of highly polarized pathogenic effector T$_H$2 (peT$_H$2) cells in the periphery, these cells have “innate-like” phenotypic characteristics, such as the expression of receptors for IL-25 and IL-33, that may allow sustained inflammation in the absence of specific antigen stimulation (9, 10).

Recent single-cell RNA sequencing studies have confirmed that such peT$_H$2 cells reside in the esophageal tissue of patients with EoE, but the limited numbers of these cells recovered precluded comprehensive assessment of the clonal relationships within this population (10). Ultimately, the signaling pathways that lead to the recruitment of peT$_H$2 cells to the esophagus and the full set of mechanisms through which these cells mediate eosinophil recruitment and chronic esophageal inflammation remain unknown. Furthermore, the clonal identities and antigen specificities of these cells have yet to be determined.

To better understand the cellular mechanisms underlying EoE, we conducted a single-cell genomic analysis of the types and functions of cells present in esophageal biopsies, duodenal biopsies, and peripheral blood of patients with EoE. We identified a population of T cells that expressed peT$_H$2 markers and was enriched in the esophageal biopsies of patients with active disease. This population upregulated expression of genes related to Th2 cytokines and lipid metabolism and also exhibited clonal expansion, consistent with antigen-dependent activation. In peripheral blood of the same patients, we detected clonotypes with a peT$_H$2 phenotype that were shared with those detected in tissue. Peripheral peT$_H$2 clonotypes that were also detected in the esophagus upregulated the gene for the esophagus-

homing receptor *GPR15*. These results suggest that GPR15+ peT_H2 cells in EoE are an antigen-specific population with enhanced esophagus homing potential.

Results

Mapping the single-cell ecosystem of eosinophilic esophagitis (EoE)

We first analyzed cells dissociated from tissue biopsies collected from ten patients with EoE. Six of these patients were diagnosed with active disease at the time of biopsy and four patients were diagnosed with disease in remission (Table S1). From each patient, we collected up to six biopsies from the esophagus and duodenum. The cells recovered from these biopsies were processed for single-cell RNA sequencing with Seq-Well (11, 12) (Figure 1A). From these tissue samples, we recovered a total of 28,816 high quality single-cell transcriptomes with greater than 500 unique genes detected (Figure S1).

The resulting gene expression matrix was processed using dimensionality reduction and was visualized with uniform manifold approximation and projection (UMAP) (13). Using graph-based clustering, we identified nine major clusters corresponding to different cell types (Figure 1B). These clusters were annotated according to the expression of marker genes and corresponded to T cells, plasma cells, granulocytes, mast cells, myeloid cells, fibroblasts, endothelial cells, esophageal epithelial cells, and duodenal epithelial cells (Figures 1C, S2, S3, Data file S1). The frequency of some cell populations varied largely between the esophagus and the duodenum; minor variation in the frequencies of these clusters in each tissue between patients may result from patient-intrinsic differences, such as age, as well as technical factors, such as variations in cell viability or the tissue dissociation process (Figures 1D, 1E). Epithelial cells were less frequent than expected in biopsies from both the esophagus and duodenum, suggesting that the larger sizes of these cells may bias against their entry into the wells on the Seq-Well arrays, resulting in an enrichment for lymphocyte populations with smaller size. Despite this technical factor, classical marker genes of EoE, including epithelial-associated transcripts such as *CCL26*, *POSTN*, and *CAPN14* were significantly upregulated in esophageal biopsies from patients with active disease, supporting that the single-cell sequencing data possessed high fidelity (Figure S4).

Eosinophils in the esophagus during active disease activate pathways regulated by NF-κB

The presence of eosinophils in the esophagus is the primary criterion for the diagnosis for EoE (1, 2, 5). At higher resolution, the cluster of granulocytes was composed primarily of eosinophils but also contained a small population of neutrophils. (Figure 2A–B). The eosinophils expressed genes for the surface markers *SIGLEC8*, *CCR3*, *PTGDR2*, and *IL5RA* as well as genes that encode for granule components, such as *CLC* (Galectin-10) and *RNASE2* (eosinophil-derived neurotoxin) (Figure 2C). In contrast, the neutrophils expressed high levels of the genes for the surface markers *CXCR2*, *FCGR3A*, and *FCGR3B* (Figure 2C). Other granule-associated proteins, including *PRG2* (major basic protein), *EPX* (eosinophil peroxidase), and *RNASE3* (eosinophil cationic protein) were not strongly expressed in eosinophils, consistent with prior reports that these proteins are primarily synthesized during eosinophil maturation and that the transcripts are not expressed in mature eosinophils (14, 15).

The fraction of eosinophils in the esophagus, calculated as the fraction of total recovered single cells, was significantly increased in patients with active disease, even though one patient in remission had a slightly elevated frequency of eosinophils (Figure 2D). An average of 4.7% of single cells recovered from the esophageal biopsies of patients with active disease were eosinophils. Eosinophils were also detected in the duodenal biopsies of all ten patients, but their frequency did not significantly differ between active disease and remission (Figure 2D). We observed a correlation between the number of eosinophils determined by histological staining and the fraction of eosinophils in our single-cell dataset, indicating concordance between the observations with single-cell RNA sequencing and with those from tissue staining (Figure 2E).

To determine how eosinophils respond to inflammatory signals produced in EoE, we identified pathways that were upregulated by eosinophils in the esophagus during active disease relative to eosinophils in the duodenum, where inflammation is not typically histologically evident (16). We found that several pro-inflammatory pathways, including “IL-2/STAT5 signaling”, “TNF signaling via NF-κB”, and “inflammatory response” were upregulated by esophageal eosinophils during active disease (Figure 2F), indicating that eosinophils recruited to the esophagus in EoE are activated by signals present in the esophagus. To elucidate gene regulatory networks that may mediate the activation of eosinophils in EoE, we utilized single-cell regulatory network inference and clustering (SCENIC) to identify gene modules that were coexpressed with transcription factors and enriched for transcription factor *cis*-regulatory motifs (17). Consistent with the analysis of transcriptional pathways, gene modules regulated by NF-κB subunits, including *NFKB1*, *NFKB2*, *REL*, and *RELB*, were among the most enriched modules in esophagus-resident eosinophils during active disease (Figure S5, Data file S2). NF-κB activation in eosinophils has previously been linked to signaling by the cytokines IL-5 and IL-33, both of which have putative roles in EoE pathogenesis, and has been demonstrated to promote the survival of eosinophils via the suppression of apoptosis (1, 5, 18–20). Interestingly, gene modules regulated by NF-κB were also elevated in the duodenum during active disease, suggesting that the inflammatory signaling present during active EoE may promote systemic activation of eosinophils, as has been observed in allergic asthma (Figure 2G) (21). Overall, these observations suggest that NF-κB is an important mediator of the activation and survival of eosinophils in EoE and provide insights into the gene regulatory networks active in eosinophils during allergic inflammation.

Phenotypic characteristics and patterns of homing marker expression differentiate esophageal and duodenal T cells

Antigen recognition by allergen-specific T cells is thought to initiate a signaling cascade that leads to the recruitment of eosinophils to the esophagus in EoE (1, 5). To determine the properties of tissue-resident T cells in EoE, we analyzed the subpopulations of T cells present in esophageal and duodenal biopsies. Tissue-specific transcriptional differences caused T cells to segregate in unsupervised analysis by their tissue of origin (Figure S6A). Therefore, we analyzed T cells from the esophagus and duodenum separately. Clustering of these cells revealed six clusters of T cells from each the esophagus and the duodenum (Figure 3A–B, Data file S3). These included clusters resembling CD8+ tissue resident

memory (Trm) cells (clusters E1, E2, D2), T_H17 cells (E5, D1), Treg cells (E3, D5), peT_H2 cells (E6), NK cells (E4, D3, D4) and proliferating Ki-67+ cells (D6) (Figure 3C). These cluster annotations demonstrated agreement with previously published single-cell RNA sequencing data for innate lymphocytes and NK cells as well as curated modules representing T helper cell phenotypes (Figure S6B–C, Data file S4) (22).

We next analyzed the phenotypic relationships between T cells in the esophagus and duodenum. In general, esophageal T cells exhibited higher levels of activation than those in the duodenum, with esophageal T_H17 cells expressing higher levels of *IL26*, *IL17A*, and *IL17F* and esophageal CD8+ cells expressing higher levels of *IFNG*, *GZMB*, and *GNLY* (Figure S6D–F, Data file S5). We also found that select homing markers were differentially expressed between esophageal and duodenal T cells. Specifically, T cells from both tissues were broadly positive for *ITGA4* and *ITGB7*, which can combine to form integrin α4β7, a canonical gut homing marker (Figure 3D) (23). In contrast, T cells in the duodenum but not the esophagus expressed *CCR9*, a marker associated with homing to the gut, and only CD4+ T cells in the esophagus expressed *GPR15*, a marker previously associated with homing to the colon or the skin (24–27). These results suggest that differential expression of these markers may promote the specific homing of T cells to either the esophagus or duodenum. Consistent with this hypothesis, we detected expression of *CCL25* and *C10orf99*, the genes that encode the ligands for CCR9 and GPR15, in only the duodenal epithelium or the esophageal epithelium, respectively (Figure 3E) (24, 25). Protein expression was confirmed by immunohistochemistry of esophageal biopsies of EoE patients, which identified GPR15-expressing lymphocytes as well as GPR15L expression concentrated in the basal epithelium (Figure 3F). Flow cytometry of T cells from esophageal biopsies derived from an additional set of EoE patients also demonstrated frequent surface expression of GPR15 on esophagus-resident memory CD4+ T cells (Figure 3G–H, S7A–C). These results suggest that GPR15 is a novel marker of esophagus homing that is selectively upregulated on CD4+ T cells in the esophagus.

peT_H2 cells are enriched in the esophagus during EoE

We next examined the relationship between esophagus-resident T cell clusters and each patient's EoE diagnosis. We found that the fraction of the peT_H2 cluster (E6), calculated as the fraction of total T cells recovered from the esophagus, was significantly higher in patients with active disease (Figure 4A). The size of cluster E6 was also correlated with the number of eosinophils detected in biopsies, suggesting a relationship between the presence of peT_H2 cells and the recruitment of eosinophils to the esophagus (Figure 4B).

To further analyze the phenotype of peT_H2 cells in EoE, we identified pathways upregulated by peT_H2 cells relative to other T cells in the esophagus. Consistent with prior studies of tissue-resident T_H2 cells in EoE and asthma, the pathways significantly upregulated in peT_H2 cells included arachidonic acid metabolism, lipid metabolism, PPAR-γ signaling, and eicosanoid production (Figure S8A–B) (10, 28). To further investigate how dysregulated lipid metabolism may mediate tissue-level inflammation in EoE, we mapped the expression of genes in peT_H2 cells directly onto a network of arachidonic acid metabolism. We identified three genes overexpressed by peT_H2 cells: *PLA2G16*, *PTGS2*, and *HPGDS*,

which together can fully process arachidonate stored in membrane-associated phospholipids to form prostaglandin-D2 (PGD2) (Figure 4C). peT_H2 cells also overexpressed the genes for a variety of enzymes involved in the processing of long-chain and very long-chain fatty acids, several of which are reported to have a specificity for arachidonic acid-derived metabolites (29–31). We also detected these features among peT_H2 cells in a single-cell dataset from a prior study of eosinophilic esophagitis as well as datasets generated from skin suction blisters of patients with atopic dermatitis and nasal scrapings of patients with chronic rhinosinusitis (10, 32, 33) (Figure S9), indicating that they represent functions of peT_H2 cells that are conserved across multiple tissues and disease contexts. These results suggest that a fundamental characteristic of tissue-resident peT_H2 cells across multiple allergic diseases is dysregulation of lipid metabolism conducive to promoting production of PGD2.

To determine to what extent peT_H2 cells in the esophagus tissue may directly mediate the recruitment and activation of eosinophils, we performed an analysis of receptor-ligand interactions to predict communication axes present between tissue-resident eosinophils and peT_H2 cells. Briefly, we employed a permutation-based approach and a database of receptor-ligand interactions to identify receptors selectively expressed on eosinophils that are paired with ligands selectively expressed by peT_H2 cells. Predicted interactions between peT_H2 cells and eosinophils included those involving the Th2 cytokines IL-13, IL-4, and IL-5 as well as interactions between eicosanoids and the DP2 receptor (*PTGDR2*) (Figure 4D). Mast cells shared expression of many of these receptors with eosinophils (Figure 4D), suggesting that similar pathways may mediate the activation of mast cells and eosinophils by peT_H2 cells in EoE. Together, these results suggest that a distinguishing characteristic of tissue-resident peT_H2 cells in EoE is altered lipid metabolism which promotes the production of PGD2 and that, in addition to T_H2 cytokines, PGD2 may play a role in mediating recruitment and activation of eosinophils in the esophagus during EoE.

Tissue-resident peT_H2 cells demonstrate a clonally expanded repertoire

We next sought to understand the clonotypic relationships represented among tissue-resident T cell phenotypes. We recovered paired TCRα and TCRβ sequences for individual T cells from nine of the ten patients in our study (34). In sum, we obtained TCRβ sequences for 50.3% of T cells, TCRα sequences for 32.5% of T cells, and both TCRβ and TCRα sequences for 21.5% of T cells (Figure S10A). All subsets of T cells demonstrated some degree of clonal expansion, indicating that these phenotypes include populations of tissue-resident memory T cells (Figure 5A–E). Clonally expanded peT_H2 cells, defined as multiple cells sharing a common alpha or beta chain CDR3 sequence, were detected in three of the four patients with active disease and with multiple TCRs recovered from the peT_H2 cluster (Figure 5F). These results indicate that the repertoire of tissue-resident peT_H2 cells in EoE exhibits clonal expansion, an important feature of an antigen-specific response.

Peripheral CRTH2+ CD161+ T cells are enriched for a peT_H2 phenotype

The surface marker CD161 has been reported to be upregulated on highly differentiated peT_H2 cells in allergy and helminth infection, and peripheral CRTH2+ CD161+ memory CD4+ T cells have been associated with EoE (9, 35, 36). To understand to what extent

the peT$_H$2 phenotype observed in the esophagus tissue of patients with active EoE is recapitulated among peripheral CRTH2+ CD4+ T cells, we obtained PBMCs from eight of the EoE patients in this study. From these samples, we isolated memory CD4+ T cells and polyclonally activated these cells *ex vivo* in a TCR-dependent manner (anti-CD3/anti-CD28 coated beads) for six hours. We then sorted three populations of memory CD4+ T cells: CRTH2+CD161+, CRTH2+CD161-, and CRTH2-CD161- (Figure 6A). Compared to patients in remission, patients with active disease had significantly higher frequencies of CRTH2+CD161- cells and a trend toward increased frequencies of CRTH2+CD161+ cells (Figure 6B).

We also processed CRTH2+CD161+, CRTH2+CD161-, and CRTH2-CD161- CD4+ T cells sorted from these eight patients for single-cell RNA sequencing. We obtained data from a total of 30,635 cells, comprising 6,664 CRTH2+CD161+ cells, 7,597 CRTH2+CD161- cells, and 16,374 CRTH2-CD161- cells. Among these cells, we identified six major clusters representing phenotypic states among these CD4+ T cells in the peripheral blood. (Figure 6C–D, Data file S6). The CRHT2+CD161- population was enriched for cells in cluster 2, and the CRTH2+CD161+ population was enriched in cells in clusters 2 and 3 (Figure 6E). These clusters did not completely align with the CRTH2+CD161- and CRTH2+CD161+ populations defined with FACS, indicating a degree of transcriptional heterogeneity within each population defined by surface protein expression. Clusters 2 and 3 expressed features typically associated with T$_H$2 cells, including the cytokines *IL4* and *IL13* (Figure 6F). Cluster 3, however, expressed the highest levels of the T$_H$2 cytokines *IL4*, *IL5*, *IL9*, and *IL13* as well as other features previously associated with a peT$_H$2 phenotype, including high levels of *HPGDS* and the transcripts for surface markers *IL17RB* and *IL1RL1* (9, 35). Taken together, these data suggest that cluster 2 contained conventional T$_H$2 (convT$_H$2) cells, and cluster 3 contained peT$_H$2 cells.

We then analyzed the expression of genes associated with tissue-resident peT$_H$2 cells in each cluster. We found that peripheral peT$_H$2 cells, but not convT$_H$2 cells, upregulated the expression of the genes associated with dysregulated lipid metabolism identified in esophagus-resident peT$_H$2 cells (Figure 6F). Interestingly, while the levels of T$_H$2 cytokines were higher among peripheral peT$_H$2 cells, the levels of these lipid metabolism-related genes were higher among tissue resident peT$_H$2 cells, suggesting that dysregulated lipid metabolism and eicosanoid synthesis is an acquired function of peT$_H$2 cells in esophageal tissue.

Peripheral convT$_H$2 and peT$_H$2 cells are clonally expanded and demonstrate convergence of TCR sequences

To assess the clonotypic relationships among peripheral CRTH2+CD4+ T cells in EoE, we recovered paired TCRα and TCRβ sequences from sorted cells (Figure S10B). We found high levels of clonal expansion among both convT$_H$2 and peT$_H$2 cells but not non-T$_H$2 cells, suggesting that these cells may be expanded by exposure to antigen during active disease (Figure 7A–B). To determine to what extent cells within a clonotype may share similar phenotypes, we examined the distribution of phenotypes present within each expanded clonotype. Strikingly, we found that nearly all expanded clonotypes demonstrated

a preference for either the convT$_H$2 phenotype or the peT$_H$2 phenotype, indicating that these phenotypes represent distinct clonal lineages, potentially associated with the recognition of distinct epitopes, that may diverge due to distinct conditions experienced during priming (Figure 7C). We also found that the diversity of TCRβ sequences among the peT$_H$2 and convT$_H$2 populations was significantly less than non-T$_H$2 cells, further indicating that these phenotypes are associated with expanded T cell clonotypes (Figure 7D).

We sought to determine to what extent distinct TCR clonotypes among the convT$_H$2 and peT$_H$2 populations may recognize common epitopes. We determined the nearest neighbor Hamming distances for all TCRβ CDR3 amino acid sequences recovered from each patient and found that clonotypes in the convT$_H$2 and peT$_H$2 populations were significantly more likely than non-T$_H$2 cells to have a nearest neighbor within a Hamming distance of one, corresponding to a single amino acid substitution, demonstrating a convergence of TCR sequences among these clonotypes (Figure 7E). We also utilized GLIPH2 analysis, which defines “specificity groups” of TCRs that are predicted to share a common epitope (37). convT$_H$2 and peT$_H$2 cells clonotypes significantly more likely than non-T$_H$2 cells to belong to a specificity group with another TCRβ sequence, further indicating that distinct clonotypes among these populations likely share common epitopes (Figure 7F). In addition, we observed that clonotypes that had a nearest neighbor Hamming distance of one or belonged to a GLIPH2 specificity group were more expanded than clonotypes without these characteristics, suggesting a dominant oligoclonal antigen-specific response (Figure S11A–B). Trends in clonal expansion, diversity, and TCR sequence convergence were more pronounced between the transcriptionally-defined convT$_H$2 and peT$_H$2 clusters than the protein-defined CRTH2+CD161- and CRTH2+CD161+ fractions obtained with FACS, indicating that the CD161 marker is neither completely sensitive nor specific for the clonally expanded peT$_H$2 transcriptional state (Figure S11C–F). Overall, these results indicate that peripheral convT$_H$2 and peT$_H$2 cells in EoE patients exhibit substantial clonotypic expansion and TCR sequence convergence, suggesting that their repertoire is selected for a defined set of epitopes.

Esophagus-resident peT$_H$2 clonotypes are present among peripheral CRTH2+ CD4+ cells and upregulate *GPR15*

To determine whether T cell clonotypes were shared among peripheral peT$_H$2 cells and esophagus-resident peT$_H$2 cells, we compared TCR usage between peT$_H$2 cells from esophageal tissue and cells from peripheral blood. We found a total of 26 cells from two patients that expressed a TCRβ or TCRα sequence that was also detected in an esophagus-resident peT$_H$2 cell, indicating that esophagus-resident peT$_H$2 clonotypes can simultaneously be detected in the tissue and among CRTH2+CD4+ cells in the peripheral blood (Figure 7G). The TCRβ CDR3 sequences of two of these clonotypes from the same patient differed by only a single amino acid substitution (Gly → Ser), suggesting these two esophagus-trafficking peT$_H$2 clonotypes likely recognized the same epitope. In total, 84.3% (22 out of 26) of peripheral cells that belonged to clonotypes detected among esophagus-resident peT$_H$2 cells had a peT$_H$2 phenotype, indicating that a subset of peripheral peT$_H$2 cells share both phenotypic and clonotypic identity with esophagus-resident peT$_H$2 cells.

To determine if any phenotypic characteristics distinguish esophagus-associated peT$_H$2 cells from other peT$_H$2 cells in peripheral blood, we determined genes that were differentially expressed between peT$_H$2 clonotypes also detected in the esophagus tissue and other peripheral peT$_H$2 cells. The gene *GPR15* was the most significantly upregulated transcript in peT$_H$2 clonotypes that were found in the esophagus tissue (Figure 7H, Data file S7). Only 1.04% of all peripheral peT$_H$2 cells had detectable *GPR15* transcript expression, but *GPR15* transcript was detected in 23% (6 out of 26) of peripheral peT$_H$2 clonotypes that were also detected in esophageal biopsies (Figure S12A–B). This result suggests that GPR15 may function to promote trafficking of peT$_H$2 cells to the esophagus during EoE and that GPR15 may serve as a marker of esophagus-associated peT$_H$2 cells in the peripheral blood of patients with EoE.

peT$_H$2 cells from patients with milk-triggered EoE demonstrate milk reactivity

Lastly, to determine to what extent esophagus-homing peT$_H$2 cells in EoE are reactive to disease-associated antigens, we obtained PBMCs from nine EoE patients with milk-triggered disease. We stimulated the cells for 22 hours with milk protein and analyzed the cells using flow cytometry (Figure S13A). The activation marker CD154 (CD40L) was used to detect antigen-reactive CD4+ T cells (38). Strikingly, antigen-reactive CD154+ T cells were significantly enriched for CRTH2+CD161+ cells relative to resting CD154- cells, indicating that a substantial fraction of peripheral peT$_H$2 cells from patients with EoE are reactive to food antigens (Figure 7I–J, S13B). In addition, GPR15 was enriched on CD154+ T cells relative to CD154- T cells and was expressed on a fraction of CD154+CRTH2+CD161+ T cells, suggesting that a subset of antigen-reactive peT$_H$2 cells may possess enhanced esophagus homing potential (Figures 7I, 7K, S13B). FFAR3, a previously reported marker for peT$_H$2 cells in EoE (10), was also enriched on CD154+ cells relative to CD154- cells but was detected on a much lower fraction of memory CD4+ cells than was GPR15 (Figure S13C). Overall, these results demonstrate that a significant fraction of peT$_H$2 clonotypes are reactive to disease-associated food antigens and confirm the association of GPR15 with antigen-reactive peT$_H$2 cells in EoE.

Discussion

Here, we have analyzed the transcriptional characteristics and TCR repertoire of peT$_H$2 cells from the esophageal biopsies, duodenal biopsies, and peripheral blood of patients with EoE. By comparing the characteristics of peT$_H$2 cells across these three compartments, we provide insight into the mechanisms that drive inflammation in EoE, including the pathways that lead to recruitment of peT$_H$2 cells to the esophagus, the abilities of these cells to mediate eosinophilic inflammation, and the clonal relationships manifest among this population.

Previous single-cell sequencing-based studies have been limited in their ability to detect eosinophils and other granulocytes because of their low RNA content and high concentration of RNAses (33). Using Seq-Well, we recovered numbers of eosinophils that correlated with their counts in clinical biopsies. We found that esophagus-resident eosinophils exhibited enhanced expression of genes regulated by NF-κB, indicating that these cells

are likely responsive to inflammatory signals produced in EoE and are active mediators of inflammation. Notably, activation of NF-κB in eosinophils has been demonstrated to increase eosinophil survival and has been associated with IL-5 and IL-33 signaling (18–20), providing mechanistic insight into the pathways influencing the activation of eosinophils during EoE.

In this study, we found expression of the marker *GPR15* to be specifically enriched on CD4+ cells in the esophagus, especially on peT$_H$2 cells. *GPR15* expression was also increased on peT$_H$2 clonotypes detected in both esophagus tissue and peripheral blood, and was found to be upregulated on milk-reactive peT$_H$2 cells in patients with milk-triggered disease. These data suggest that GPR15 expression promotes esophagus homing of peT$_H$2 cells in EoE, and that GPR15 may serve as a marker for esophagus-trafficking peT$_H$2 cells in the peripheral blood of patients with EoE. Further investigation of this finding in increased numbers of patients with a range of clinical presentations could enhance understanding of how this population influences the pathology of EoE.

We have also demonstrated the existence of clonal expansion among peT$_H$2 cells in both the esophagus tissue and the periphery. In addition, we detected expanded clonotypes that exhibit convergence of TCR sequences. This observation suggests the presence of an oligoclonal response by multiple clonotypes that adopt a shared phenotype and may be dominated by a small number of epitopes within a patient. Interestingly, clonotypes typically demonstrated a preference for one of the peT$_H$2 or convT$_H$2 transcriptional states, suggesting that each phenotype represents a distinct set of clonal lineages that may diverge due to the nature of the particular antigens recognized or due to distinct conditions experienced during priming. Lastly, we found that the peT$_H$2 phenotype is highly enriched among milk-reactive T cells in patients with milk-triggered disease, further suggesting that the dominant epitopes recognized by peT$_H$2 cells in EoE are derived from disease-associated allergens. Future studies involving the validation of allergen-specific peT$_H$2 cells in EoE patients could enable the identification of the precise allergen-derived epitopes recognized by peT$_H$2 cells in EoE and allow the diagnosis of EoE-related food triggers without empirical evaluation of avoidance diets, a significant unmet clinical need.

peT$_H$2 cells were originally described as a pro-eosinophilic subset of T$_H$2 cells distinct from conventional T$_H$2 cells with an enhanced ability to produce the cytokine IL-5 (39, 40). Additional characteristics of peT$_H$2 cells have been proposed across a wide spectrum of allergic diseases, including increased expression of the surface markers CD161, IL-25R, IL-33R, CCR8, and FFAR3, the enzyme HPGDS, and the transcription factor PPAR-γ (9, 10, 35, 41, 42). In this study, we have highlighted previously undescribed characteristics associated with this phenotype, including an upregulation of genes associated with lipid metabolism and expression of a complete synthetic pathway for the eicosanoid PGD2. Interestingly, our analysis of cognate receptor-ligand pairings transcriptionally active in the esophageal tissue (Figure 4D) predicted that peT$_H$2 cells directly influence tissue-resident eosinophils through the production of PGD2, a function that was also detected in peripheral peT$_H$2 cells but not convT$_H$2 cells. These findings suggest that the pathogenicity of peT$_H$2 cells may result directly from their production of PGD2 and motivates further studies analyzing the differentiation and behavior of peT$_H$2 cells. Such studies could inform

mechanisms and interventional treatments for EoE and for other allergic disorders. In addition, EoE is a reported adverse event for patients undergoing oral immunotherapy (OIT) for food allergy (43–45), suggesting that similar characteristics may develop among food allergen-specific CD4+ T cells in patients undergoing OIT.

Allergen-induced inflammation in EoE has been suggested to be driven by the recognition of antigen by peT$_H$2 cells (1, 5). This hypothesis is further supported by the detection of clonal expansion and convergence of TCR sequences among tissue-resident and peripheral peT$_H$2 cells in this study. We observed that these peT$_H$2 cells express the cytokines IL-5 and IL-13, which promote inflammation in EoE by driving eosinophil recruitment and contributing to epithelial barrier dysfunction, respectively (1, 5, 6). In addition, we report evidence that esophagus-resident peT$_H$2 cells are also involved in the production of PGD2. The release of PGD2 may promote inflammation by generating a positive feedback loop involving the chemotaxis and activation of eosinophils, mast cells, and peT$_H$2 cells themselves. This positive feedback loop may be further amplified by other inflammatory signals such as IL-33 release from damaged epithelial cells, which induces further activation of *IL1RL1*-expressing eosinophils and peT$_H$2 cells. In addition to these factors, group 2 innate lymphoid cells (ILC2s), which have also been observed in the esophageal biopsies of EoE patients (46), may contribute to inflammation in EoE through the production of IL-5 and IL-13. We did not detect ILC2s in our single-cell RNA sequencing; this absence may have resulted from the rarity of these cells combined with the relatively small biopsies available in this study.

In summary, we have profiled key allergic mediators present in the esophageal and duodenal biopsies of EoE patients, including tissue-resident eosinophils and peT$_H$2 cells. We find that tissue-resident peT$_H$2 cells are a clonally expanded population associated with a distinct phenotypic state involving eicosanoid signaling. These cells are enriched among food allergen-reactive CD4+ T cells in EoE patients and exhibit an upregulation of GPR15, which promotes esophagus homing. Further knowledge of the development of peT$_H$2 cells, their interactions with other allergic mediators, and the antigens recognized by these cells is vital to advancing our understanding, diagnosis, and treatment of EoE and other allergic and eosinophilic diseases.

Materials and Methods

Study design

The objective of this study was to understand the types and functions of cells present in esophageal biopsies and peripheral blood of patients with EoE and to determine how these cells are altered in active disease versus remission. Cells from tissue biopsies and peripheral blood were analyzed with paired single-cell RNA and TCR sequencing as well as flow cytometry. The study was approved by the Institutional Review Board of Partners Healthcare (protocol nos. 2010P002087 and 2011P001159) at Massachusetts General Hospital. Sample size was determined based on the availability of biopsy samples. Researchers performing the single-cell RNA sequencing and flow cytometry experiments were blinded to the patient diagnoses. Diagnoses of active EoE and EoE in remission were provided by physicians and considered factors such as the number of eosinophils per high power field and other features

of microscopic pathology, as well as the appearance of the esophagus upon endoscopy, as assessed by EREFS scoring (47), and current patient symptoms (Table S1).

Esophagus biopsy collection and processing

Up to six biopsies in total from the proximal, mid, and distal esophagus or duodenum were collected from each patient. Biopsies were minced with scalpels into fragments of ~1 mm^2 and processed into a single-cell suspension by performing two subsequent digestions with Collagenase A (2 mg/mL) and DNase I (100 μg/mL) (both from Millipore-Sigma, St. Louis, MO) in RPMI medium (Gibco, Waltham, MA) for 40 minutes at 37°C. Remaining fragments of tissue were removed by centrifugation (100*g* for 2 minutes), and the supernatant cell suspension was filtered through a 70-micron cell strainer and washed twice with cold staining buffer (PBS + 0.5% BSA + 2mM EDTA) before further use.
For analysis of biopsy samples with flow cytometry, single-cell suspensions from multiple patients were pooled and labeled with BUV395-conjugated anti-CD3 (clone UCHT1), APC-Cy7-conjugated anti-CD4 (RPA-T4), PE-Cy7-conjugated anti-CD45RA (HI100) (all from BD Biosciences, San Jose, CA), Live/Dead Fixable Blue stain (L23105; Thermo Fisher, Waltham, MA), and PE-conjugated anti-GPR15 (SA302A10; BioLegend, San Diego, CA). Samples were analyzed with a BD Fortessa X-20 instrument (BD Biosciences) and analyzed with FlowJo v10 software.

Activation and sorting of peripheral blood T cell populations

Cryopreserved PBMC from 8 of the 10 patients included in the tissue-resident single-cell analysis were thawed, and memory $CD4^+$ T cells were isolated with the EasySep human memory $CD4^+$ T cell enrichment kit (Stemcell Technologies, Vancouver, BC, Canada). T cells were cultured in AIM-V medium (Gibco) for 6 hours at a density of 2×10^6 in 0.5 mL medium per well in 48-well plates, with human T-Activator CD3/CD28 beads (Thermo Fisher) in a 1:3 ratio of beads to T cells. After harvesting, the cells were labeled with BUV395-conjugated anti-CD3, APC-Cy7-conjugated anti-CD4, PE-Cy7-conjugated anti-CD45RA, PerCP-Cy5.5-conjugated anti-CRTH2 (BM16; BD Biosciences), eFluor450-conjugated anti-CD161 (HP-3G10; Thermo Fisher), and Live/Dead Fixable Blue stain. Live $CD3^+CD4^+CD45RA^-$ $CRTH2^+CD161^+$, $CRTH2^+CD161^-$, and $CRTH2^-CD161^-$ T cells were sorted with a FACSAria Fusion instrument (BD Biosciences).

Analysis of peripheral blood milk-reactive $CD4^+$ T cells

Cryopreserved PBMC from 9 patients with milk- or dairy-triggered EoE (no overlap with the patients included in the single-cell analysis) were thawed and cultured in AIM-V medium for 22 hours, with or without 75 μg/ml cow's milk protein (M7409; Millipore-Sigma), at a density of 5×10^6 in 1 ml medium per well in 24-well plates. FITC-conjugated anti-CD154 (clone TRAP1; BD Biosciences) was added to the cultures (20 μL/well) for the last 3 hours. After harvesting, the cells were labeled with BUV395-conjugated anti-CD3, APC-Cy7-conjugated anti-CD4, PE-Cy7-conjugated anti-CD45RA, FITC-conjugated anti-CD154, PerCP-Cy5.5-conjugated anti-CRTH2, eFluor450-conjugated anti-CD161, PE-conjugated anti-GPR15, APC-conjugated anti-FFAR3 (LS-C214200; LSBio, Seattle, WA), and Live/Dead Fixable Blue stain. Flow cytometry data were collected with a FACSAria Fusion instrument, and analyzed with FlowJo v10 software.

Single-cell RNA-sequencing

Single-cell suspensions from esophageal biopsies, duodenal biopsies, and sorted subsets of peripheral blood CD4+ memory T cells were processed for single-cell RNA sequencing using the Seq-Well platform with second strand chemistry, as previously described (11, 12). Libraries were barcoded and amplified using the Nextera XT kit (Illumina, San Diego, CA) and were sequenced on a Novaseq 6000 (Illumina).

Paired single-cell TCR sequencing and analysis

Paired TCR sequencing and read alignment was performed as described in Tu et al (34). Briefly, whole-transcriptome amplification product for each sample was enriched for TCR transcripts using biotinylated probes for the human *TRAC* and *TRBC* regions and magnetic streptavidin beads. The enriched product was further amplified using human V-region primers and Nextera sequencing handles. Libraries were then sequenced on an Illumina MiSeq or Nextseq using single-end reads. CDR3 consensus sequences were aligned as outlined previously. To prevent collisions between cell barcodes that may originate from Hamming distance correction, we aggregated all molecules with the same CDR3 sequence, clustered the unique molecular identifiers (UMI) of these sequences according to Hamming distance with a maximum distance of 2, and retained the single UMI with the greatest number of total reads. UMI with less than an 80% CDR3 consensus frequency were then excluded from analysis. GLIPH2 analysis was performed as described in Huang et al. using the default parameters and version 2 of the provided reference for human data (37).

Single-cell Data Processing and Visualization

Raw read processing of single-cell RNA sequencing reads was performed according to Macosko et al (48). Briefly, reads were aligned to the hg38 reference genome and collapsed by cell barcode and UMI. For the dataset generated from esophageal and duodenal biopsies, cells with less than 500 unique genes detected and genes detected in fewer than 5 cells were filtered out, and for the dataset of peripheral CD4+ memory T cells, cells with less than 900 unique genes detected and genes detected in fewer than 5 cells were filtered out. First, the data for each cell was log-normalized to account for library size. We then selected variable genes with log-mean expression values greater than 0.1 and a dispersion of greater than 1. The ScaleData function in Seurat was used to regress out the number of UMI and percentage of mitochondrial genes in each cell and to scale the data to unit variance using a Poisson model. Next, principle components analysis was performed and the top ten components were used to generate a UMAP visualization. Clusters were determined using the FindClusters function in Seurat. A small number of cells recovered from esophageal biopsies clustered with duodenal epithelial cells and were excluded from further analysis.

Correction for ambient RNA contamination using SoupX

Ambient RNA correction was performed using SoupX v0.3.0 as described in Young et al (49) with minor modifications. Cell contamination fractions were estimated using the genes *KRT4, KRT5, KRT13, KRT15*, and *KRT6A* in non-esophageal epithelial cells for samples from the esophagus and the genes *IGHA1*, *IGHA2*, *IGHM*, *IGJ*, and *IGKC* in non-plasma cells for samples from the duodenum. These estimates were refined using the

calculateContaminationFraction to fit lowess curves between the number of UMI for each cell and the estimated contamination fraction. Adjusted counts were rounded to integers to preserve the count nature of the data. After ambient RNA correction was complete, the data was reprocessed and re-visualized as described above.

Doublet removal and individual cell type analysis

Clusters representing a single cell type were first processed as described in the "single-cell data processing and data visualization" section above. Doublet clusters were then identified as clusters that strongly expressed marker genes associated with more than one cell population and were discarded. Preprocessing steps were then performed one additional time prior to beginning analysis.

Gene module and pathway enrichment analysis

Gene sets for innate T cell subsets and NK cells were generated by determining the top 30 differentially expressed genes by each subset in the data from Gutierrez-Arcelus et al., were obtained from MSigDB (50), or were curated according to standard marker genes for T helper cells. Gene scores were obtained using the AddModuleScore function in Seurat. For analysis of eosinophil transcriptomes, MSigDB pathways in the Hallmarks collection were analyzed, and for analysis of peT$_H$2 cells, MSigDB pathways in the KEGG and BIOCARTA collections were analyzed.

SCENIC analysis of eosinophils

The python package pySCENIC version 0.9.18 was used to infer gene regulatory networks in eosinophils (17, 51). The input into the pySCENIC workflow was the gene counts matrix for cells classified as eosinophils and the RcisTarget database containing transcription factor motif scores for gene promoters around transcription start sites in the hg38 genome. Transcription factor modules upregulated in eosinophils during active disease were identified by performing a two-sided Wilcoxon rank-sum test on the AUCell scores for each transcription factor module between eosinophils from esophageal biopsies of patients with active disease and eosinophils from the duodenal biopsies of all patients.

Immunohistochemical staining

Formalin-fixed paraffin-embedded biopsy sections were prepared using standard protocols. Heat-mediated epitope retrieval was performed at 97 degrees C for 20 minutes with pH 6 citrate buffer, using the ThermoFisher PT module. Slides were run on the ThermoFisher 360 Autovision IHC stainer. The run consisted of: Endogenous peroxidase blocking: 10 minutes, Protein block: 30 minutes, Primary antibody: 60 minutes, Labeled polymer: 30 minutes, DAB: 5 minutes. The primary antibodies used were: GPR15 (HPA-013775, Millipore-Sigma) and C10orf99 (PA5–62266, ThermoFisher).

Receptor-ligand pathway analysis

To identify receptor-ligand interactions between peT$_H$2 cells and eosinophils in the esophagus tissue, we utilized pathways annotated as "known" and "literature supported" from a published database of receptor-ligand pairs (52). We aimed to identify receptor-

ligand pairs in which the receptor was selectively upregulated on eosinophils relative to other cells from esophageal biopsies and the ligand was selectively upregulated by peT$_H$2 cells relative to other T cell subsets. We defined eosinophils or peT$_H$2 cells as "expressing" a receptor or ligand if at least ten percent of the cells in that cluster expressed transcript for that receptor or ligand. For all pathways in which both eosinophils and peT$_H$2 cells expressed the corresponding receptor and ligand, we then defined a "receptor score" and "ligand score" equal to average normalized expression value for the gene encoding the receptor or ligand. We then generated a null distribution for receptor scores and ligand scores by performing 10,000 permutations of the cell type labels among cells recovered from esophageal biopsies and recalculating both receptor scores and ligand scores. We then used this null distribution to calculate p-values for both receptor scores and ligand scores, and we defined the p-value for each receptor-ligand pair as the maximum of the p-value for the receptor score and the p-value for the ligand score.

Reanalysis of literature datasets

Data from Wen et al., Bangert et al., and Ordovas-Montanes et al. was obtained from GSE126250, GSE153760, and the Supplementary Data of Ordovas-Montanes et al. For Bangert et al., data from skin suction blisters of patients with atopic dermatitis was used. For all datasets, non-T cells and T cells with under 500 unique genes detected were excluded. Data from Bangert et al. and Ordovas-Montanes et al. was processed using the methodology described above. Data from Wen et al. was first normalized by computing transcripts per million. Variable genes were then selected using the FindVariableGenes function in Seurat and scaled using the ScaleData function in Seurat. After performing PCA, a number of principle components were selected from an elbow plot and used to generate UMAP projections for each dataset. For all data sets, clusters were then determined using the FindClusters function in Seurat. A small cluster of cells labeled as T cells in the Ordovas-Montanes et al. dataset appeared to represent eosinophils and was excluded from analysis.

Statistical analysis

Statistical analysis was performed in the R software, version 3.5.1. The specific parametric and nonparametric statistical tests are indicated in the figure legends. P-values < 0.05 were considered statistically significant. For differential gene expression analysis, genes with an adjusted p-value < 0.001 and an average log-fold change of greater than 0.25 were considered statistically significant.

Supplementary Material

Refer to Web version on PubMed Central for supplementary material.

Acknowledgements:

We thank our patients and their families who generously gave their time and participation, as well as Maria Davila and Astrid Swensen, the clinical coordinators of this study.

Funding: This work was supported in part by the Koch Institute Support (core) NIH Grant P30-CA14051 from the National Cancer Institute, as well as the Koch Institute - Dana-Farber/Harvard Cancer Center Bridge

Project. This work was also supported by the Food Allergy Science Initiative at the Broad Institute and the NIH (1UL1TR001102). The MGH Department of Pathology Flow and Image Cytometry Research Core, which provided assistance with FACS, obtained funding from the National Institutes of Health Shared Instrumentation program (1S10OD012027-01A1, 1S10OD016372-01, 1S10RR020936-01, and 1S10RR023440-01A1).

References and Notes

1. Furuta GT, Katzka DA, Eosinophilic esophagitis. N. Engl. J. Med. 373, 1640–1648 (2015). [PubMed: 26488694]
2. Davis BP, Rothenberg ME, Mechanisms of disease of eosinophilic esophagitis. Annu. Rev. Pathol. Mech. Dis. 11, 365–93 (2016).
3. Gonsalves N, Yang GY, Doerfler B, Ritz S, Ditto AM, Hirano I, Elimination diet effectively treats eosinophilic esophagitis in adults; Food reintroduction identifies causative factors. Gastroenterology. 142, 1451–1459.e1 (2012). [PubMed: 22391333]
4. Davis BP, Rothenberg ME, Mechanisms of Disease of Eosinophilic Esophagitis. Annu. Rev. Pathol. 11, 365–93 (2016). [PubMed: 26925500]
5. Hill DA, Spergel JM, The immunologic mechanisms of eosinophilic esophagitis. Curr. Allergy Asthma Rep. 16, 1–15 (2016). [PubMed: 26677109]
6. Rochman M, Azouz NP, Rothenberg ME, Epithelial origin of eosinophilic esophagitis. J. Allergy Clin. Immunol. 142, 10–23 (2018). [PubMed: 29980278]
7. Sherrill JD, KC K, Blanchard C, Stucke EM, Kemme KA, Collins MH, Abonia JP, Putnam PE, Mukkada VA, Kaul A, Kocoshis SA, Kushner JP, Plassard AJ, Karns RA, Dexheimer PJ, Aronow BJ, Rothenberg ME, Analysis and expansion of the eosinophilic esophagitis transcriptome by RNA sequencing. Genes Immun. 15, 361–369 (2014). [PubMed: 24920534]
8. Kottyan LC, Rothenberg ME, Genetics of eosinophilic esophagitis. Mucosal Immunol. 10, 580–588 (2017). [PubMed: 28224995]
9. Mitson-Salazar A, Yin Y, Wansley DL, Young M, Bolan H, Arceo S, Ho N, Koh C, Milner JD, Stone KD, Wank SA, Prussin C, Hematopoietic prostaglandin D synthase defines a proeosinophilic pathogenic effector human TH2 cell subpopulation with enhanced function. J. Allergy Clin. Immunol. 137, 907–918.e9 (2016). [PubMed: 26431580]
10. Wen T, Aronow BJ, Rochman Y, Rochman M, KC K, Dexheimer PJ, Putnam P, Mukkada V, Foote H, Rehn K, Darko S, Douek D, Rothenberg ME, Single-cell RNA sequencing identifies inflammatory tissue T cells in eosinophilic esophagitis. J. Clin. Invest. 129, 2014–2028 (2019). [PubMed: 30958799]
11. Gierahn TM, Wadsworth MH, Hughes TK, Bryson BD, Butler A, Satija R, Fortune S, Love JC, Shalek AK, Seq-Well: portable, low-cost RNA sequencing of single cells at high throughput. Nat. Methods. 14, 395–398 (2017). [PubMed: 28192419]
12. Hughes TK, Wadsworth MH, Gierahn TM, Do T, Weiss D, Andrade PR, Ma F, de Andrade Silva BJ, Shao S, Tsoi LC, Ordovas-Montanes J, Gudjonsson JE, Modlin RL, Love JC, Shalek AK, Second-Strand Synthesis-Based Massively Parallel scRNA-Seq Reveals Cellular States and Molecular Features of Human Inflammatory Skin Pathologies. Immunity. 53, 878–894.e7 (2020). [PubMed: 33053333]
13. McInnes L, Healy J, Melville J, UMAP: Uniform Manifold Approximation and Projection for Dimension Reduction. arXiv (2018) (available at http://arxiv.org/abs/1802.03426).
14. Gruart V, Truong MJ, Plumas J, Zandecki M, Kusnierz JP, Prin L, Vinatier D, Capron A, Capron M, Decreased expression of eosinophil peroxidase and major basic protein messenger RNAs during eosinophil maturation. Blood. 79, 2592–7 (1992). [PubMed: 1375105]
15. Bystrom J, Amin K, Bishop-Bailey D, Analysing the eosinophil cationic protein - a clue to the function of the eosinophil granulocyte. Respir. Res. 12, 10 (2011). [PubMed: 21235798]
16. Kaur S, Rosen JM, Kriegermeier AA, Wechsler JB, Kagalwalla AF, Brown JB, Utility of Gastric and Duodenal Biopsies during Follow-up Endoscopy in Children with Eosinophilic Esophagitis. J. Pediatr. Gastroenterol. Nutr. 65, 399–403 (2017). [PubMed: 28118289]
17. Aibar S, González-Blas CB, Moerman T, Huynh-Thu VA, Imrichova H, Hulselmans G, Rambow F, Marine J-C, Geurts P, Aerts J, van den Oord J, Atak ZK, Wouters J, Aerts S, SCENIC: single-cell

regulatory network inference and clustering. Nat. Methods. 14, 1083–1086 (2017). [PubMed: 28991892]

18. Schwartz C, Willebrand R, Huber S, Rupec RA, Wu D, Locksley R, Voehringer D, Eosinophil-specific deletion of IκBα in mice reveals a critical role of NF-κB-induced Bcl-xLfor inhibition of apoptosis. Blood. 125, 3896–3904 (2015). [PubMed: 25862560]
19. Bouffi C, Rochman M, Zust CB, Stucke EM, Kartashov A, Fulkerson PC, Barski A, Rothenberg ME, IL-33 Markedly Activates Murine Eosinophils by an NF-κB–Dependent Mechanism Differentially Dependent upon an IL-4–Driven Autoinflammatory Loop. J. Immunol. 191, 4317–4325 (2013). [PubMed: 24043894]
20. Judd LM, Heine RG, Menheniott TR, Buzzelli J, O'Brien-Simpson N, Pavlic D, O'Connor L, Al Gazali K, Hamilton O, Scurr M, Collison AM, Mattes J, Allen KJ, Giraud AS, Elevated IL-33 expression is associated with pediatric eosinophilic esophagitis, and exogenous IL-33 promotes eosinophilic esophagitis development in mice. Am. J. Physiol. Liver Physiol. 310, G13–G25 (2016).
21. Hoppenot D, Malakauskas K, Lavinskiene S, Sakalauskas R, p-STAT6, PU.1, and NF-κB are involved in allergen-induced late-phase airway inflammation in asthma patients. BMC Pulm. Med. 15, 122 (2015). [PubMed: 26466682]
22. Gutierrez-Arcelus M, Teslovich N, Mola AR, Polidoro RB, Nathan A, Kim H, Hannes S, Slowikowski K, Watts GFM, Korsunsky I, Brenner MB, Raychaudhuri S, Brennan PJ, Lymphocyte innateness defined by transcriptional states reflects a balance between proliferation and effector functions. Nat. Commun. 10, 1–15 (2019). [PubMed: 30602773]
23. Agace WW, Tissue-tropic effector T cells: Generation and targeting opportunities. Nat. Rev. Immunol. 6, 682–692 (2006). [PubMed: 16932753]
24. Griffith JW, Sokol CL, Luster AD, Chemokines and chemokine receptors: positioning cells for host defense and immunity. Annu. Rev. Immunol. 32, 659–702 (2014). [PubMed: 24655300]
25. Suply T, Hannedouche S, Carte N, Li J, Grosshans B, Schaefer M, Raad L, Beck V, Vidal S, Hiou-Feige A, Beluch N, Barbieri S, Wirsching J, Lageyre N, Hillger F, Debon C, Dawson J, Smith P, Lannoy V, Detheux M, Bitsch F, Falchetto R, Bouwmeester T, Porter J, Baumgarten B, Mansfield K, Carballido JM, Seuwen K, Bassilana F, A natural ligand for the orphan receptor GPR15 modulates lymphocyte recruitment to epithelia. Sci. Signal. 10 (2017), doi:10.1126/scisignal.aal0180.
26. Habtezion A, Nguyen LP, Hadeiba H, Butcher EC, Leukocyte trafficking to the small intestine and colon. Gastroenterology. 150, 340–354 (2016). [PubMed: 26551552]
27. Xiong L, Dean JW, Fu Z, Oliff KN, Bostick JW, Ye J, Chen ZE, Mühlbauer M, Zhou L, Ahr-Foxp3-RORγt axis controls gut homing of CD4 $^{+}$ T cells by regulating GPR15. Sci. Immunol. 5, eaaz7277 (2020). [PubMed: 32532834]
28. Tibbitt CA, Stark JM, Martens L, Ma J, Mold JE, Deswarte K, Oliynyk G, Feng X, Lambrecht BN, De Bleser P, Nylén S, Hammad H, Arsenian Henriksson M, Saeys Y, Coquet JM, Single-Cell RNA Sequencing of the T Helper Cell Response to House Dust Mites Defines a Distinct Gene Expression Signature in Airway Th2 Cells. Immunity. 51, 169–184.e5 (2019). [PubMed: 31231035]
29. Kuwata H, Hara S, Role of acyl-CoA synthetase ACSL4 in arachidonic acid metabolism. Prostaglandins Other Lipid Mediat. 144, 106363 (2019). [PubMed: 31306767]
30. Shindou H, Hishikawa D, Nakanishi H, Harayama T, Ishii S, Taguchi R, Shimizu T, A single enzyme catalyzes both platelet-activating factor production and membrane biogenesis of inflammatory cells: Cloning and characterization of acetyl-CoA:lyso-PAF acetyltransferase. J. Biol. Chem. 282, 6532–6539 (2007). [PubMed: 17182612]
31. Tang W, Bunting M, Zimmerman GA, McIntyre TM, Prescott SM, Molecular cloning of a novel human diacylglycerol kinase highly selective for arachidonate-containing substrates. J. Biol. Chem. 271, 10237–10241 (1996). [PubMed: 8626589]
32. Bangert C, Rindler K, Krausgruber T, Alkon N, Thaler FM, Kurz H, Ayub T, Demirtas D, Fortelny N, Vorstandlechner V, Bauer WM, Quint T, Mildner M, Jonak C, Elbe-Bürger A, Griss J, Bock C, Brunner PM, Persistence of mature dendritic cells, T H 2A, and Tc2 cells characterize clinically resolved atopic dermatitis under IL-4Rα blockade. Sci. Immunol 6, eabe2749 (2021). [PubMed: 33483337]

33. Ordovas-Montanes J, Dwyer DF, Nyquist SK, Buchheit KM, Vukovic M, Deb C, Wadsworth MH, Hughes TK, Kazer SW, Yoshimoto E, Cahill KN, Bhattacharyya N, Katz HR, Berger B, Laidlaw TM, Boyce JA, Barrett NA, Shalek AK, Allergic inflammatory memory in human respiratory epithelial progenitor cells. Nature. 560, 649–654 (2018). [PubMed: 30135581]
34. Tu AA, Gierahn TM, Monian B, Morgan DM, Mehta NK, Ruiter B, Shreffler WG, Shalek AK, Love JC, TCR sequencing paired with massively parallel 3′ RNA-seq reveals clonotypic T cell signatures. Nat. Immunol. 20, 1692–1699 (2019). [PubMed: 31745340]
35. Wambre E, Bajzik V, DeLong JH, O'Brien K, Nguyen Q-A, Speake C, Gersuk VH, DeBerg HA, Whalen E, Ni C, Farrington M, Jeong D, Robinson D, Linsley PS, Vickery BP, Kwok WW, A phenotypically and functionally distinct human TH2 cell subpopulation is associated with allergic disorders. Sci. Transl. Med. 9, eaam9171 (2017). [PubMed: 28768806]
36. de Ruiter K, Jochems SP, Tahapary DL, Stam KA, König M, van Unen V, Laban S, Höllt T, Mbow M, Lelieveldt BPF, Koning F, Sartono E, Smit JWA, Supali T, Yazdanbakhsh M, Helminth infections drive heterogeneity in human type 2 and regulatory cells. Sci. Transl. Med 12, eaaw3703 (2020). [PubMed: 31894102]
37. Huang H, Wang C, Rubelt F, Scriba TJ, Davis MM, Analyzing the Mycobacterium tuberculosis immune response by T-cell receptor clustering with GLIPH2 and genome-wide antigen screening. Nat. Biotechnol, 1–9 (2020). [PubMed: 31919444]
38. Chattopadhyay PK, Yu J, Roederer M, A live-cell assay to detect antigen-specific CD4+ T cells with diverse cytokine profiles. Nat. Med. 11, 1113–1117 (2005). [PubMed: 16186817]
39. Upadhyaya B, Yin Y, Hill BJ, Douek DC, Prussin C, Hierarchical IL-5 Expression Defines a Subpopulation of Highly Differentiated Human Th2 Cells. J. Immunol. 187, 3111–3120 (2011). [PubMed: 21849680]
40. Mitson-Salazar A, Prussin C, Pathogenic effector Th2 cells in allergic eosinophilic inflammatory disease. Front. Med. 4, 165 (2017).
41. Micossé C, von Meyenn L, Steck O, Kipfer E, Adam C, Simillion C, Seyed Jafari SM, Olah P, Yawlkar N, Simon D, Borradori L, Kuchen S, Yerly D, Homey B, Conrad C, Snijder B, Schmidt M, Schlapbach C, Human "TH9" cells are a subpopulation of PPAR-γ+ TH2 cells. Sci. Immunol 4, eaat5943 (2019). [PubMed: 30658968]
42. Islam SA, Chang DS, Colvin RA, Byrne MH, McCully ML, Moser B, Lira SA, Charo IF, Luster AD, Mouse CCL8, a CCR8 agonist, promotes atopic dermatitis by recruiting IL-5+TH2 cells. Nat. Immunol. 12, 167–177 (2011). [PubMed: 21217759]
43. Burk CM, Dellon ES, Steele PH, Virkud YV, Kulis M, Burks AW, Vickery BP, Eosinophilic esophagitis during peanut oral immunotherapy with omalizumab. J. Allergy Clin. Immunol. Pract. 5, 498–501 (2017). [PubMed: 28017628]
44. Lucendo AJ, Arias Á, Tenias JM, Relation between eosinophilic esophagitis and oral immunotherapy for food allergy: A systematic review with meta-analysis. Ann. Allergy, Asthma Immunol. 113, 624–629 (2014). [PubMed: 25216976]
45. Cafone J, Capucilli P, Hill DA, Spergel JM, Eosinophilic esophagitis during sublingual and oral allergen immunotherapy. Curr. Opin. Allergy Clin. Immunol. 19, 350–357 (2019). [PubMed: 31058677]
46. Doherty TA, Baum R, Newbury RO, Yang T, Dohil R, Aquino M, Doshi A, Walford HH, Kurten RC, Broide DH, Aceves S, Group 2 innate lymphocytes (ILC2) are enriched in active eosinophilic esophagitis. J. Allergy Clin. Immunol. 136, 792–794 (2015). [PubMed: 26233928]
47. Wechsler JB, Bolton SM, Amsden K, Wershil BK, Hirano I, Kagalwalla AF, Eosinophilic Esophagitis Reference Score Accurately Identifies Disease Activity and Treatment Effects in Children. Clin. Gastroenterol. Hepatol. 16, 1056–1063 (2018). [PubMed: 29248734]
48. Macosko EZ, Basu A, Satija R, Nemesh J, Shekhar K, Goldman M, Tirosh I, Bialas AR, Kamitaki N, Martersteck EM, Trombetta JJ, Weitz DA, Sanes JR, Shalek AK, Regev A, McCarroll SA, Highly parallel genome-wide expression profiling of individual cells using nanoliter droplets. Cell. 161, 1202–1214 (2015). [PubMed: 26000488]
49. Young MD, Behjati S, SoupX removes ambient RNA contamination from droplet based single cell RNA sequencing data (2018), doi:10.1101/303727.

50. Liberzon A, Subramanian A, Pinchback R, Thorvaldsdóttir H, Tamayo P, Mesirov JP, Bateman A, Databases and ontologies Molecular signatures database (MSigDB) 3.0. Bioinformatics. 27, 1739–1740 (2011). [PubMed: 21546393]

51. Van de Sande B, Flerin C, Davie K, De Waegeneer M, Hulselmans G, Aibar S, Seurinck R, Saelens W, Cannoodt R, Rouchon Q, Verbeiren T, De Maeyer D, Reumers J, Saeys Y, Aerts S, A scalable SCENIC workflow for single-cell gene regulatory network analysis. Nat. Protoc. 15, 2247–2276 (2020). [PubMed: 32561888]

52. Ramilowski JA, Goldberg T, Harshbarger J, Kloppmann E, Lizio M, Satagopam VP, Itoh M, Kawaji H, Carninci P, Rost B, Forrest ARR, A draft network of ligand–receptor-mediated multicellular signalling in human. Nat. Commun. 6, 7866 (2015). [PubMed: 26198319]

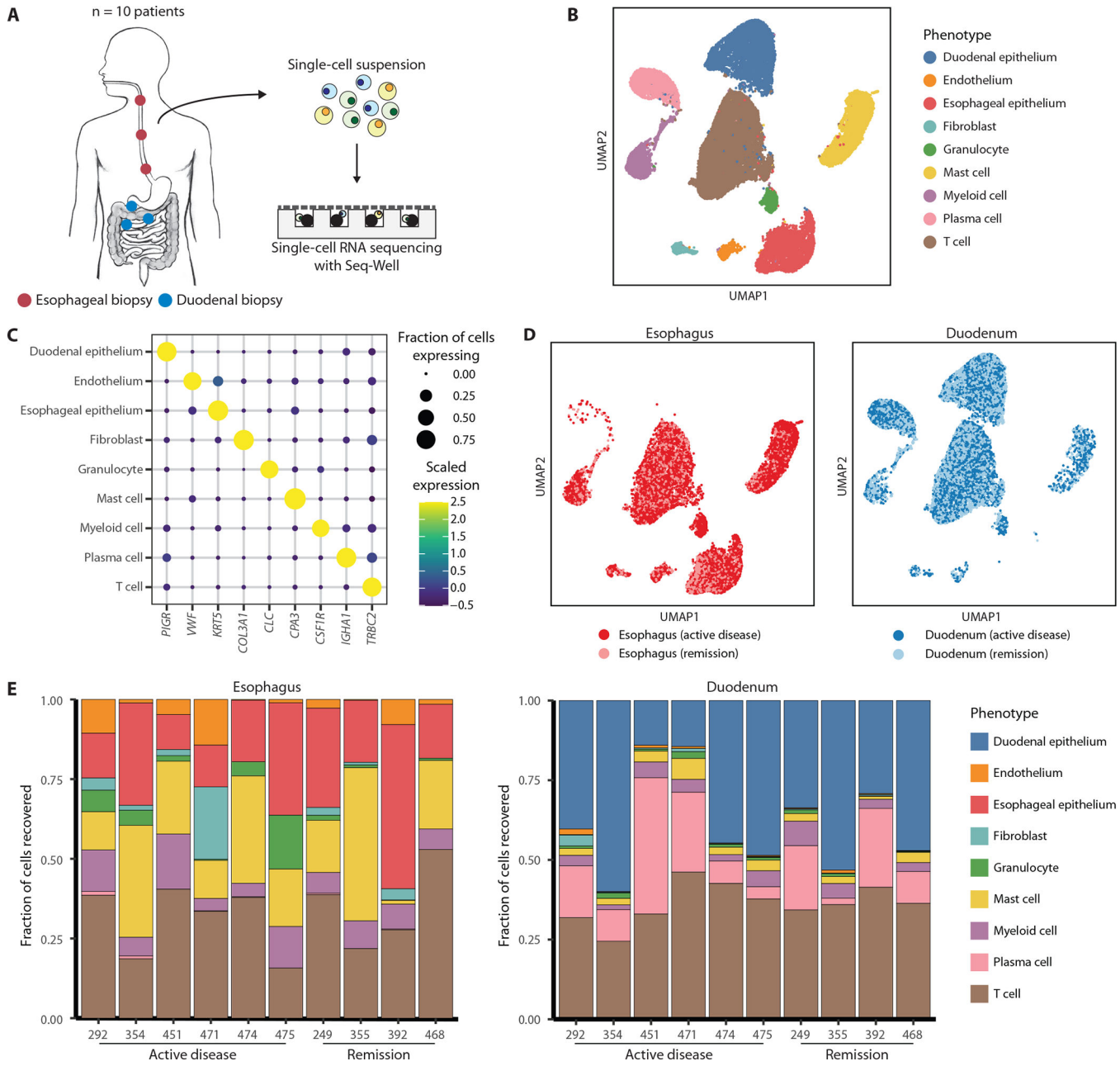

Figure 1. Single-cell RNA sequencing of esophageal and duodenal biopsies of EoE patients.

(**A**) Schematic of biopsy processing pipeline. Biopsies from ten EoE patients (six with active disease, four in remission) were enzymatically dissociated into single-cell suspensions and processed for single-cell RNA sequencing using Seq-Well. (**B**) UMAP projection of 28,816 cells obtained from the esophageal and duodenal biopsies of ten EoE patients, colored by cell phenotype. (**C**) Dot plots of select marker genes for each cell phenotype, displaying average expression and frequency of expression for each gene. (**D**) UMAP projections of cells obtained from esophageal and duodenal biopsies, colored by tissue and patient diagnosis. (**E**) Bar plots depicting relative frequencies of cell phenotypes from the esophageal and duodenal biopsies of each patient.

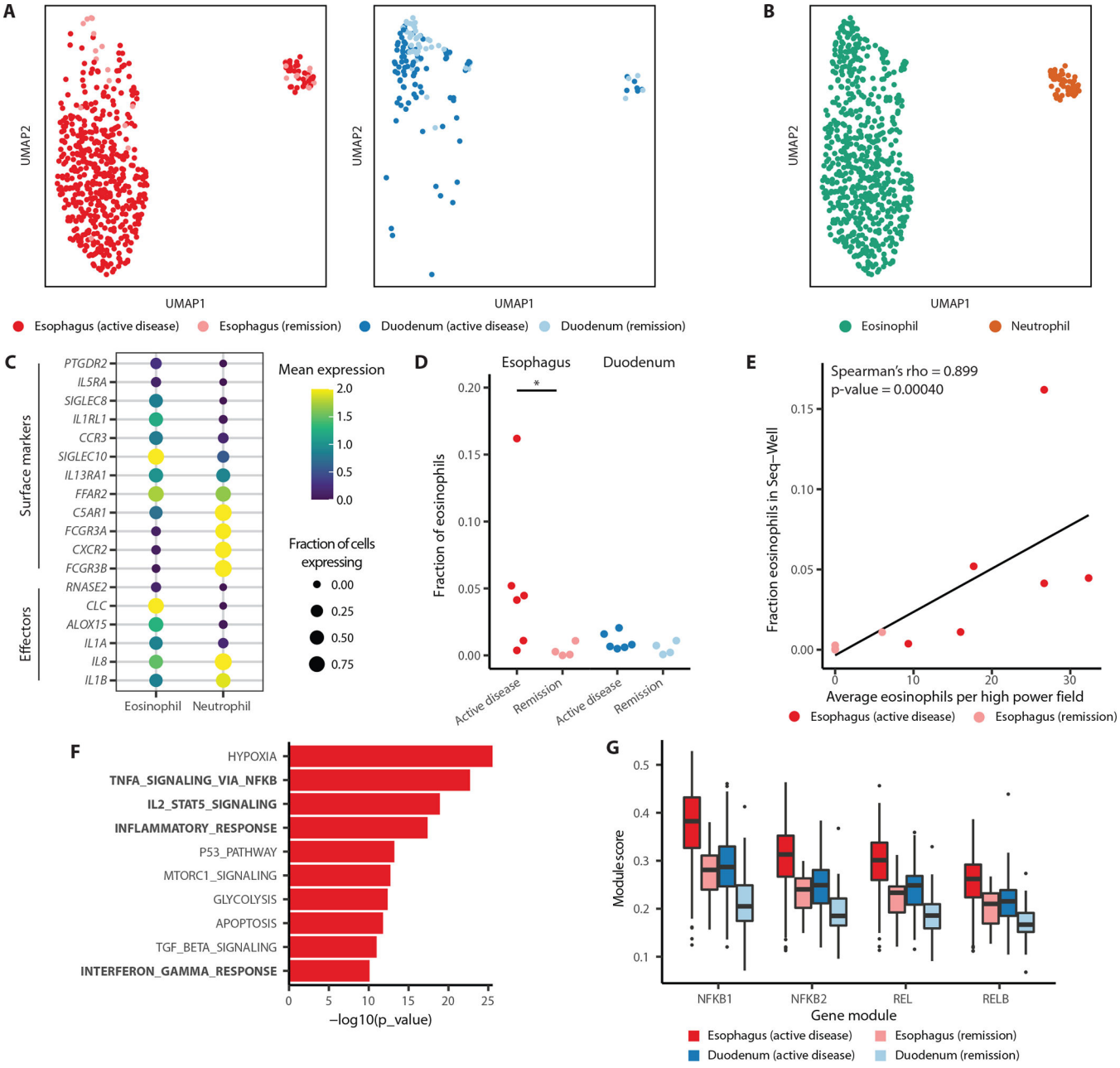

Figure 2. Eosinophils are enriched and activated in the esophagus during active disease.

(**A**) UMAP projection of granulocyte cluster colored by tissue and disease status (n = 679 cells). (**B**) UMAP projection of granulocyte cluster, colored by type of granulocyte. (**C**) Dot plots of select surface markers and inflammatory effectors expressed by eosinophils and neutrophils, displaying average expression and frequency of expression for each gene. (**D**) Fraction of cells in single-cell data that were classified as eosinophils from esophageal or duodenal biopsies of patients in disease or remission. P-values were computed using a two-sided Wilcoxon rank-sum test (*P < 0.05). (**E**) Correlation between number of eosinophils per high power field in esophagus tissue determined with histological staining and fraction of eosinophils in esophagus single-cell data. Spearman's correlation coefficient

and the associated p-value are shown. (**F**) Pathways upregulated in eosinophils present in the esophageal tissue of patients with active disease relative to eosinophils in the duodenum. P-values are calculated with a two-sided Wilcoxon rank-sum test and are adjusted with Bonferroni correction. (**G**) Transcription factor module scores produced by SCENIC for modules regulated by subunits of NF-κB.

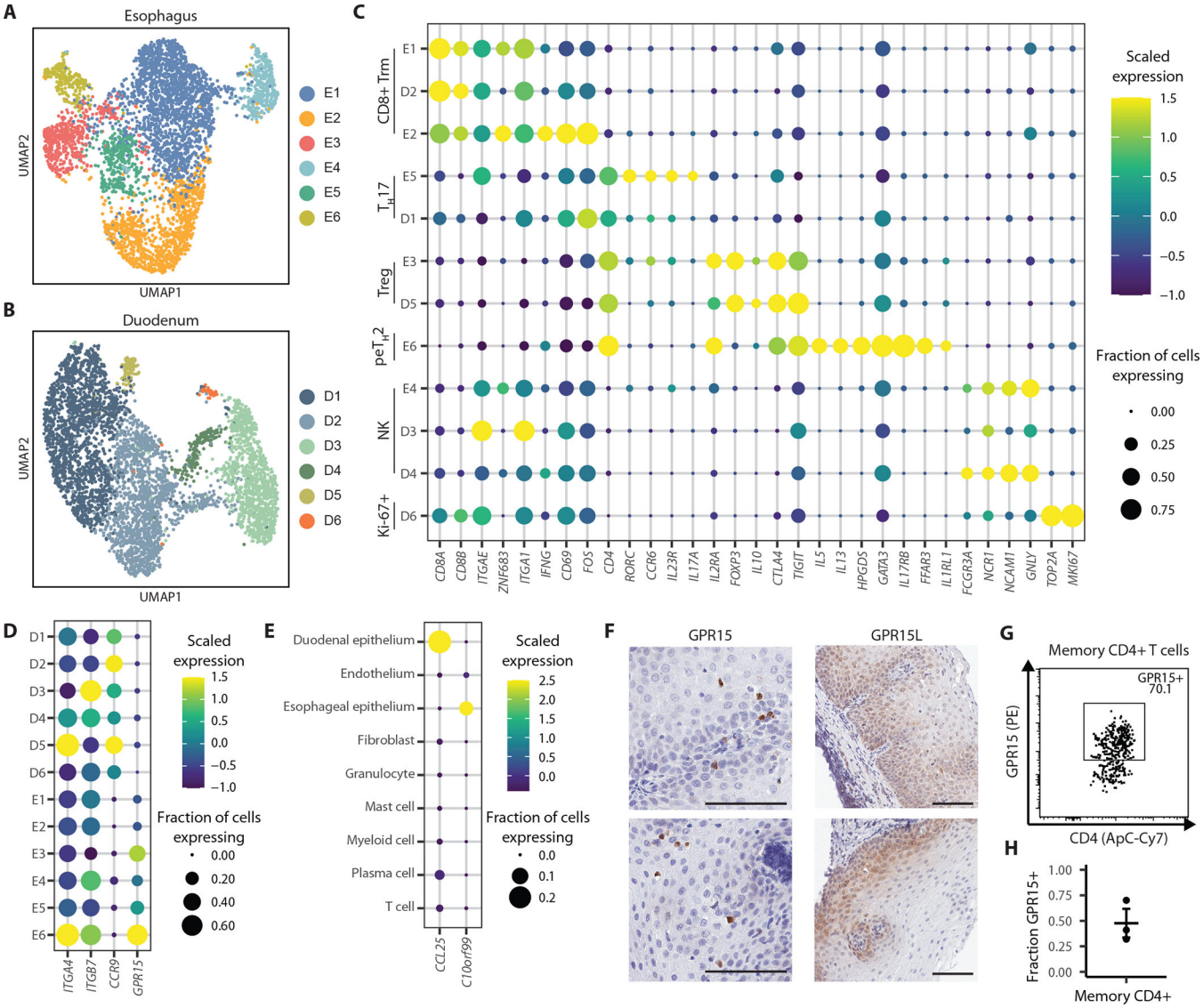

Figure 3. T cell phenotypes present in the esophagus and duodenum.

(**A**) UMAP projection of T cells recovered from esophagus biopsies, colored by phenotypic cluster (n = 4,423 cells). (**B**) UMAP projection of T cells recovered from duodenum biopsies, colored by phenotypic cluster (n = 4,781 cells). (**C**) Dot plot of select genes in tissue-resident T cell clusters, displaying scaled expression and frequency of expression for each gene. (**D**) Dot plot of select homing markers in esophagus and duodenum T cell clusters. (**E**) Dot plot of *CCL25* and *C100orf99*, the ligands for CCR9 and GPR15, in tissue-resident cell phenotypes. (**F**) Immunohistochemical staining for GPR15 and GPR15L in the esophageal biopsies of EoE patients. Scale bar: 200 μm. Results representative of n=3 patients. (**G**) GPR15 expression on memory CD4+ T cells isolated from esophageal biopsies of EoE patients, as measured by flow cytometry. Results representative of n=3 experiments. (**H**) Fraction of memory CD4+ T cells expressing from esophageal biopsies expressing GPR15+.

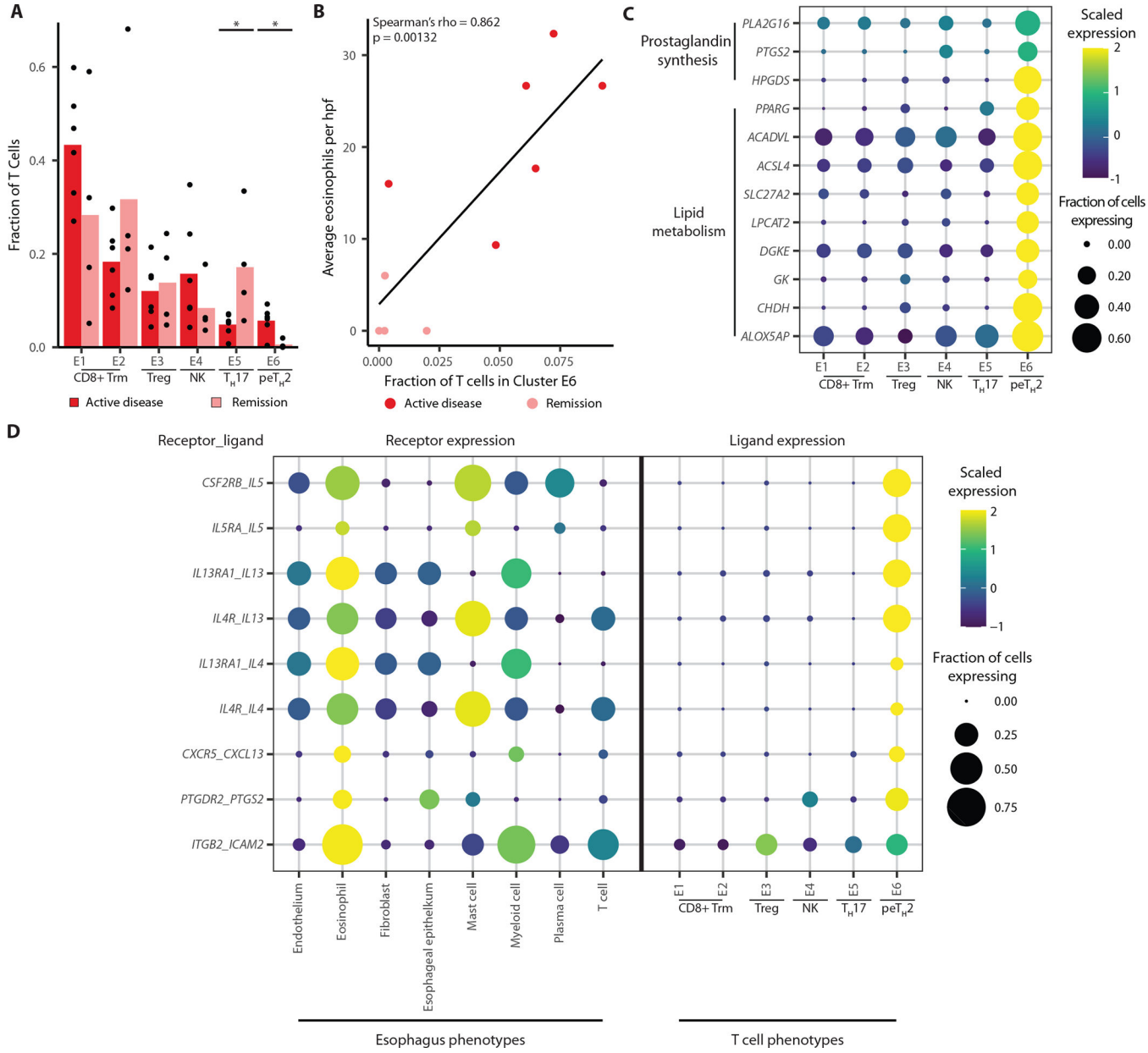

Figure 4. Properties of peT$_H$2 cells in the esophagus of patients with EoE.

(**A**) Relative size of each esophagus T cell cluster by patient and diagnosis. P-value was computed using a two-sided Wilcoxon rank-sum test (*P < 0.05). (**B**) Correlation between fraction of T cells in cluster E6 and number of eosinophils per high-power field (hpf). Spearman's correlation coefficient and the associated p-value are shown. (**C**) Dot plot showing the expression of genes associated with prostaglandin synthesis or lipid metabolism in each esophagus T cell cluster. (**D**) Ligand-receptor pathway analysis presenting the expression of receptors and ligands in pathways determined to be selectively upregulated between eosinophils and peT$_H$2 cells. All pathways shown are determined to be statistically significant (Methods).

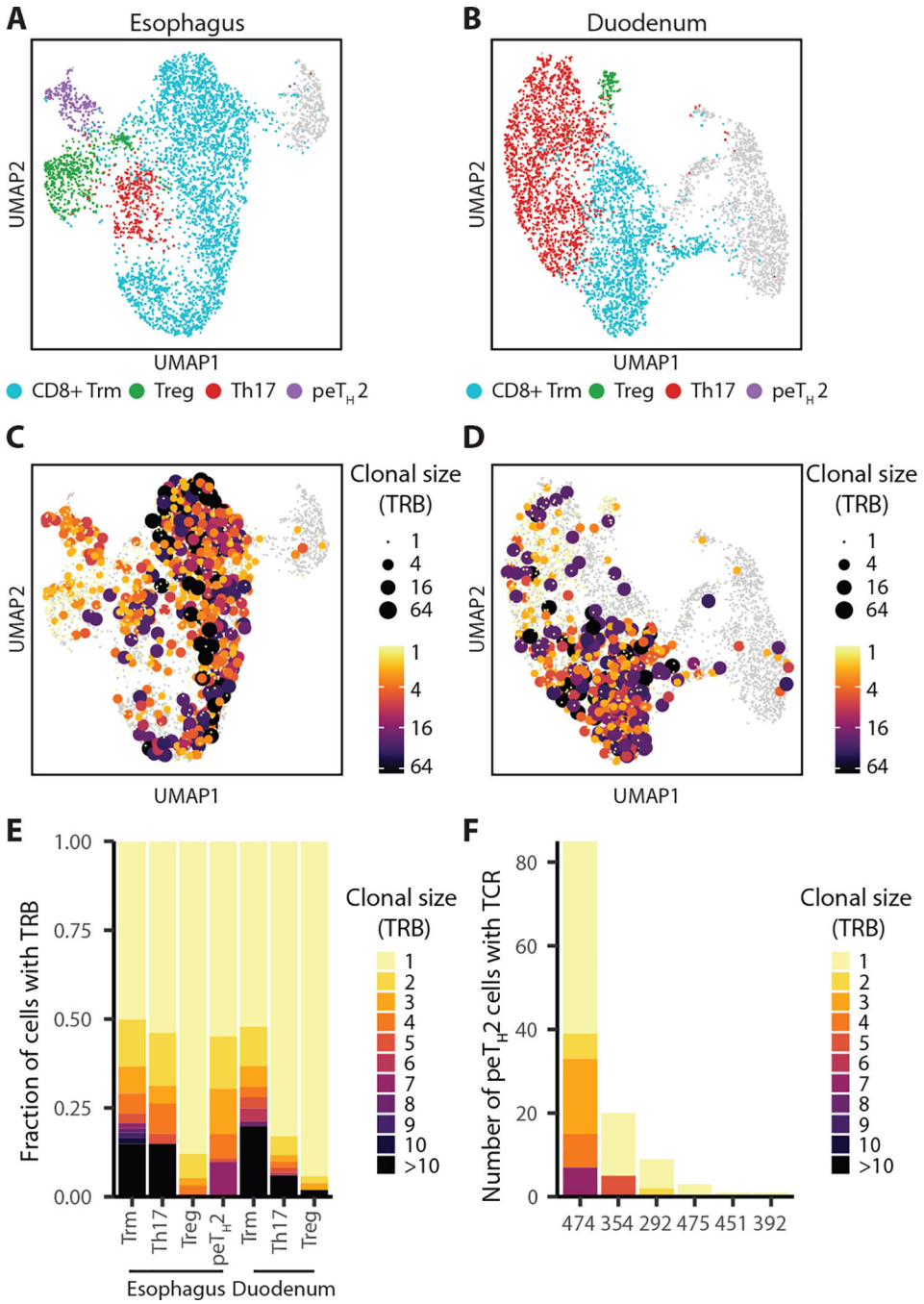

Figure 5. Clonotypic relationships of T cells in the esophagus and duodenum.

(**A**) UMAP projection of phenotypes present among esophageal T cells and (**B**) duodenal T cells. (**C**) Clonal size of esophageal T cells and (**D**) duodenal T cells mapped onto corresponding UMAP projections. Clonal size is defined as the number of cells from a given patient that share a given TRB sequence. (**E**) Stacked bar plot of clonal size of each phenotype. (**F**) Bar plot of clonal size of peT$_H$2 cells in each patient.

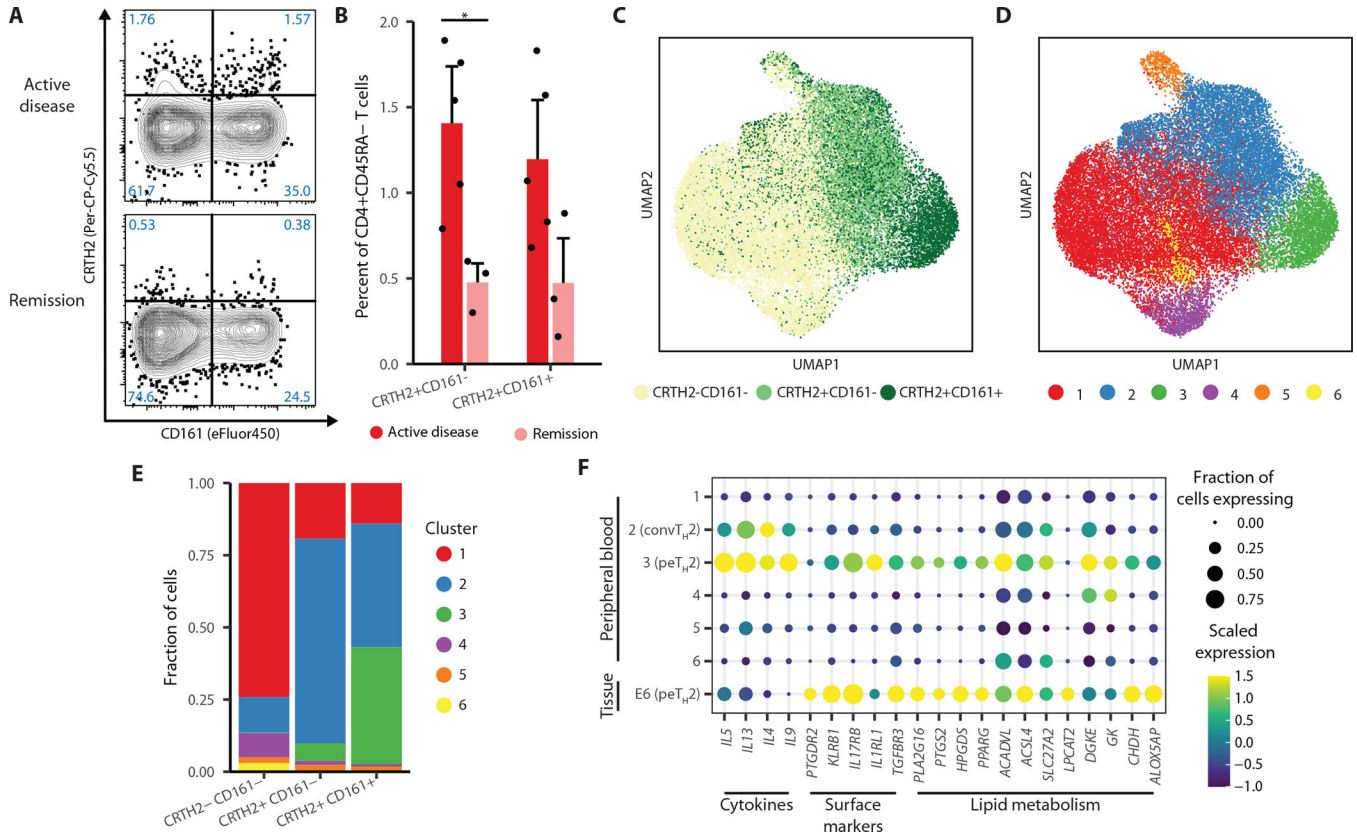

Figure 6. Comparisons between peripheral and esophagus-resident peT$_H$2 phenotypes.

(**A**) Representative staining of CRTH2 and CD161 from peripheral blood of EoE patients in disease or remission. (**B**) Percentage of CRTH2+CD161+ and CRTH2+CD161- among memory CD4+CD45RA- T cells, as determined by flow cytometry. P-values are calculated using a one-sided Wilcoxon rank-sum test (*P < 0.05). (**C**) UMAP projection of sorted CRTH2-CD161-, CRTH2+CD161-, and CRTH2+CD161+ cells, colored by sort fraction (n = 30,635 cells; 8 patients). (**D**) UMAP projection of sorted cells colored by phenotypic cluster. (**E**) Distribution of phenotypic clusters within each sort fraction. (**F**) Dot plot of peT$_H$2-associated genes in T cells from peripheral blood CD4+ T cells and cluster E6 from esophageal biopsies.

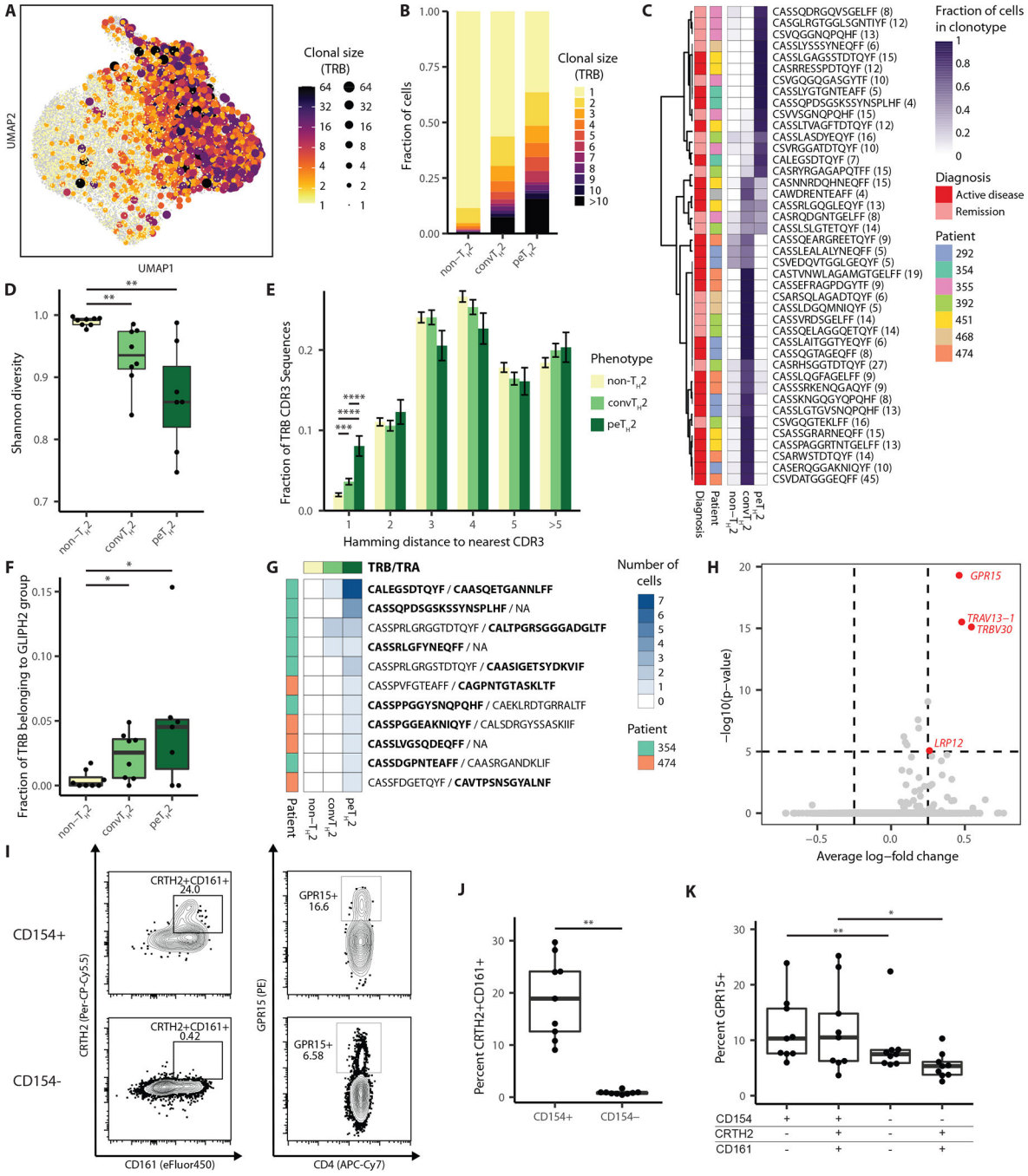

Figure 7. TCR repertoire of peripheral convT$_H$2 and peT$_H$2 cells.

(**A**) Clonal size, calculated using TCRβ, overlaid on UMAP plot. (**B**) Distribution of clonal size among non-T$_H$2, convT$_H$2, and peT$_H$2 phenotypes. (**C**) Distribution of non-T$_H$2, convT$_H$2, and peT$_H$2 phenotypes within expanded clonotypes. Up to the seven most expanded clonotypes recovered from each patient are displayed, provided they consist of greater than 3 cells. Heatmap is colored according to fraction of cells in that clonotype with a given phenotype. (**D**) Shannon diversity of non-T$_H$2, convT$_H$2, and peT$_H$2 cells. Samples with fewer than 10 TCRβ sequences recovered are excluded. P-values are calculated using

a two-sided Wilcoxon rank-sum test (**P < 0.01). (**E**) Distribution of nearest-neighbor Hamming distance between CDR3 sequences in each phenotype. P-values are calculated using a two-sided chi-squared proportion test (***P < 0.001, ****P < 0.0001). (**F**) Fraction of TCRβ sequences in each phenotype that are related to another TCRβ sequence from the same patient by GLIPH2. Samples with fewer than 10 TCRβ sequences recovered are excluded. P-values are calculated by a one-sided Wilcoxon rank-sum test (*P < 0.05). (**G**) peT_H2 clonotypes shared between the peripheral blood and the esophagus. Heatmap presents the distribution of phenotypes present in peripheral blood for each clonotype. Sequences highlighted in bold were shared between the esophagus and peripheral blood; other sequences are paired with these sequences in either location. (**H**) Genes upregulated by clonotypes detected in esophagus tissue relative to all other peripheral peT_H2 cells. P-values are calculated using a two-sided Wilcoxon rank-sum test and are adjusted with Bonferroni correction. (**I**) Representative staining of CD154+ and CD154- memory CD4+ cells from patients with milk-triggered disease. (**J**) Frequency of CRTH2+CD161+ cells on CD154+ and CD154- cells after culture with milk antigen. P-values were calculated using a paired two-sided Wilcoxon rank-sum test (**P < 0.01) (**K**) Frequency of GPR15 expression on memory T cell subsets after culture with milk antigen. P-values were calculated using a paired two-sided Wilcoxon rank-sum test (*P < 0.05, **P < 0.01).